EVALUATION ON TURBULENT MODEL IN LARGE EDDY SIMULATION OF TURBULENT FLOW AROUND A WALL-MOUNTED CUBE IN A CHANNEL

N.S. Park[1] and S.C. Ko[*2]

채널 내 부착된 입방체 장애물 주위 유동에 관한 LES 난류모델의 영향 평가

박 남 섭,[1] 고 상 철[*2]

In engineering application of large eddy simulation, there are still questions as follows grid dependency on numerical results, the effect of upwind scheme against a calculation instability, appropriate boundary conditions dealing with turbulence fluctuation and the performance of SGS models. In this study, in order to develop the LES to the engineering application, large eddy simulation was carried out to investigate the effect of upwind scheme, turbulent subgrid model and the grid dependancy of the flow around a wall-mounted cube in a channel at Re=40,000 based on cubic height and bulk mean velocity. The computed velocities, turbulence quantities, separation and reattachment length were evaluated compared with the experimental results of R. Matinuzzi and C. Tropea.

Key Words : Large Eddy Simulation, Cubic Obstacle, Smagorinsky model, Lagrangian Dynamic Model, Upwind Scheme

1. INTRODUCTION

A large eddy simulation (LES) is becoming an accurate method of simulating complex turbulent flows in an engineering problem. In the LES, the large scales of flow structure are resolved while small scales are modeled. The rationale behind this method is based on two observations: most of turbulent energy is carried by the large structures, and the small scale eddies are more isotropic and universal. Therefore, LES may be more general and less geometry dependent than the simulation based on the Reynolds averaged model. Recently, the LES has been applied to unsteady flows and three-dimensional separated flows. However, there are still some practical problems when the LES apply to engineering problems. One of the serious concerns in the LES is a computational cost. Though we believe that the computational cost of LES is much smaller than that of a direct simulation in high Reynolds number case. There are still questions for the LES of a turbulent flows in complex geometry as follows grid dependency on numerical results, the effect of upwind scheme against a calculation instability, appropriate boundary conditions dealing with turbulence fluctuation and the performance of SGS(sub-grid scale) models.

To estimate these questions, the LES has been applied to simulate turbulent flow around a cubic obstacle mounted on a channel surface (see Fig. 1) using the standard Smagorinsky model and the Lagrangian dynamic model with a coarse mesh resolution.

The prediction of flow separation is important in designing fluid machinery. This object is a typical structure, which disturbs boundary layers, generates separations and promotes turbulence. In addition, there is a numerical difficulty at the corner of the cubic obstacle such that a wiggle from the corner boundary induces

접수일: 2008년 5월 21일, 심사완료일: 2008년 9월 18일.
1 유한대학 기계공학과
2 정회원, 전주대학교 기계자동차공학과
* Corresponding author, E-mail: scko@jj.ac.kr

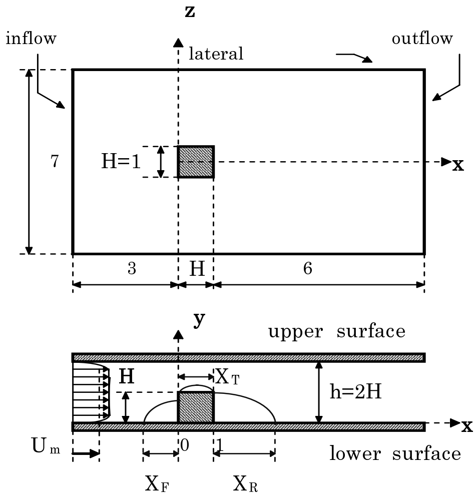

Fig. 1 Geometry of configuration

numerical errors and instability. For this reason upwind schemes are often adopted to suppress wiggles as a practical technique. In this research, the influence of the upwind scheme on prediction of averaged and instantaneous velocity fields is investigated, and grid-dependency is also discussed.

A simulation at Reynolds number Re=40000, based on the incoming bulk velocity (U_m) and cube height (H), is presented. Computational results are compared with the experiments conducted by R. Matinuzzi and C. Tropea[1].

2. Mathematical Formulation

For the LES of an incompressible flow, the governing equations consist of the filtered continuity and Navier-Stokes equations, which are given by

$$\frac{\partial \overline{u_i}}{\partial x_i} = 0 \tag{1}$$

$$\frac{\partial \overline{u_i}}{\partial t} + \frac{\partial (\overline{u_i}\,\overline{u_j})}{\partial x_j} = -\frac{\partial \overline{p}}{\partial x_i} + \frac{1}{Re}\frac{\partial^2 \overline{u_i}}{\partial x_j \partial x_j} - \frac{\partial \tau_{ij}}{\partial x_j} \tag{2}$$

Here, u_1, u_2, u_3 (or u, v, w) are the velocities in x_1 (streamwise), x_2 (normal), x_3 (spanwise) directions (or x, y, z) respectively, and p is the pressure. An over-bar symbol denotes the filtered value. All variables are nondimensionalized by the incoming bulk velocity U_m and obstacle height H. The Reynolds number is defined as $Re=U_mH/\nu$, where ν is a kinetic viscosity. In equation (2), the effect of the subgrid scale fluctuation is expressed only by a SGS stress τ_{ij} :

$$\tau_{ij} = \overline{u_i u_j} - \overline{u_i}\,\overline{u_j} \tag{3}$$

A trace of the SGS stress can be included in the pressure, but the rest needs to be modeled, for example, by a Smagorinsky model[2] as follows:

$$\tau^*_{ij} = \tau_{ij} - \frac{1}{3}\delta_{ij}\tau_{kk} = -2(C_s\overline{\triangle})^2|\overline{S}|\overline{S_{ij}}_{(4)} \tag{4}$$

$$\overline{S_{ij}} = \frac{1}{2}\left(\frac{\partial \overline{u_i}}{\partial x_j} + \frac{\partial \overline{u_j}}{\partial x_i}\right), |\overline{S}| = \sqrt{2\overline{S_{ij}}\,\overline{S_{ij}}} \tag{5}$$

where, Δ is the characteristic length of the filter defined by the grid size(h_1, h_2, h_3) in the directions, x_1, x_2, and x_3.

$$\Delta = f \cdot (\Delta x_1 \Delta x_2 \Delta x_3)^{1/3} \tag{6}$$

In the present case, we used the model constant C_s(called Smagorinsky constant) with 0.1 and the wall damping function was introduced near the wall in the form by van Driest[3]:

$$f = 1 - \exp(-y^+/25) \tag{7}$$
$$y^+ = \frac{u_\tau y_p}{\nu}, u_\tau = \sqrt{\tau_w/\rho}$$

Here, y_p, y^+ are the distance from the wall and the wall coordinate. u_τ is the wall shear velocity determined by the wall shear stress τ_w and the fluid density ρ.

A dynamic SGS model(DSM) proposed by Germano et al.[4] is now recognized as an alternative SGS model which avoids the ad hoc treatment on the Smagorinsky constant C_s and the length scale Δ. DSM uses a test filter larger than the grid filter that is assumed in the equation (1,2) and related with the grid size given by equation (6). When applying the Smagorinsky model to the both SGS stresses, the following relation is derived:

$$L_{ij} = 2(C_s\Delta)^2 M_{ij} \tag{8}$$

$$L_{ij} = T_{ij} - \widetilde{\tau_{ij}} = \widetilde{\overline{u_i}\,\overline{u_j}} - \widetilde{\overline{u_i}}\,\widetilde{\overline{u_j}} \tag{9}$$

$$M_{ij}=\overline{\triangle}^2\left(\alpha^2|\tilde{\overline{S}}|\tilde{\overline{S}}_{ij}-\widetilde{|\overline{S}|\overline{S}_{ij}}\right) \tag{10}$$

$$\alpha=\frac{\tilde{\overline{C}}_s\tilde{\overline{\triangle}}}{\overline{C}_s\overline{\triangle}} \tag{11}$$

where, tilde(~) denotes the test filter and α is a ratio of the characteristic lengths of the two filters. Here, it is noted that L_{ij} can be calculated without model. Therefore unknown values of the Smagorinsky model ($C_s\Delta$) can be 'dynamically' determined. Using a least square approach suggested by Lilly[5], the model constant can be estimated as

$$(C_s\Delta)^2=-\frac{1}{2}\frac{<L_{ij}M_{ij}>}{<M_{ij}M_{ij}>} \tag{12}$$

Numerically, equation (12) may become a negative value, which means a negative viscosity to introduce the numerical instability. For avoiding this problem in previous researches, an averaging operation denoted by < > is applied to a homogeneous direction.

In the present case, however, there are no homogeneous directions to do averaging operation. Thus we adopt the Lagrangian dynamic model(LDSM) suggested by Meneveau, et al.[6]. The Lagrangian model is derived such that the error in Germano's identity can be minimized along fluid trajectories. This procedure leads to a pair of relaxation transport equations that carry the statistics forward in the Lagrangian time. Using the Lagrangian dynamic model, $(C_s\Delta)^2$ in the equation (8) is given by

$$(C_s\Delta)^2=-\frac{1}{2}\frac{I_{LM}}{I_{MM}} \tag{13}$$

$$I_{LM}=\int_{-\infty}^{\infty}L_{ij}M_{ij}(z(t'),f')\,W(t-f')\,dt' \tag{14}$$

$$I_{MM}=\int_{-\infty}^{\infty}M_{ij}M_{ij}(z(t'),f')\,W(t-f')\,dt' \tag{15}$$

Here, using an exponential weighting function,

$$W(t-f')=\frac{\exp[-(t-f')/T]}{T} \tag{16}$$

The integrals of equation (14,15) have the solutions of the following relaxation equations

$$\frac{DI_{LM}}{Dt}=\frac{1}{T}(L_{ij}M_{ij}-I_{LM}) \tag{17}$$

$$\frac{DI_{MM}}{Dt}=\frac{1}{T}(M_{ij}M_{ij}-I_{MM}) \tag{18}$$

The time-scale T can be defined by

$$T=C_t\overline{\Delta}(I_{LM})^{-1/4} \tag{19}$$

According to the previous research of Tsubokura[7], C_t=2.0 is adopted in this work. Dynamic SGS model requires the filtering operations explicitly for calculating the test filtered quantities. A volume filter is quantities by the Simpson's method for numerical integration, and then the formulation of the finite difference method is derived as

$$\begin{aligned}\tilde{\overline{f}}&=\overline{f}+\frac{\tilde{\triangle}^2}{24}.\nabla^2\overline{f}+O(\tilde{\triangle}^4)\\&=\overline{f}_i+\frac{\gamma^2}{24}.(\overline{f}_{i+1}-2\overline{f}_i+\overline{f}_{i-1})+O(\tilde{\Delta}^4)\end{aligned} \tag{20}$$

where, $\gamma(=\tilde{\Delta}/h)$ is a ratio of the filter width $\tilde{\Delta}$ to the grid size h. According to the recommendation[8] in the channel flow of the LES, α=2 and $\gamma=\sqrt{6}$ are adopted in this research.

3. NUMERICAL METHOD

For descretizing the governing equations, the finite volume method[9] is used on a staggered grid, where the velocity components are located at the cell faces and the pressure are located at the cell center. A time marching procedure is performed by a SMAC method. The governing equations are analyzed numerically using a third order Runge-Kutta method[10] in time and a second order central difference scheme in space is adapted. When the computational grid is not fine enough, the central difference scheme for convection terms may produce a wiggle near the corner of obstacle. It is difficult to avoid such a problem in high Reynolds number flows. Therefore, the upwind schemes, such as QUICK scheme, are introduced in order to remove such wiggles. The upwind scheme induces some numerical errors. To minimize the influence of numerical errors, the upwind scheme is applied only in the upward area. A fully developed turbulent channel flow was specified instantaneously at an inlet at each time step. Periodic boundary condition is used for the spanwise direction (x-y plane). At the solid wall, supplementing the mesh resolution, we adopted an artificial condition by Spalding's law:

$$F(u^+,y^+) = u^+ - y^+ + e^{-\kappa B}\left[e^{\kappa u^+} - 1 - (\kappa u^+) - \frac{(\kappa u^+)^2}{2} - \frac{(\kappa u^+)^3}{6}\right] = 0 \tag{21}$$

where, k=0.4, B=5.5 are adopted and u^+ is velocity at the distance y_p from the wall. At the outlet section, a convective boundary condition is used[11]:

$$\frac{\partial \overline{u_i}}{\partial t} + U_b \frac{\partial \overline{u_i}}{\partial x} = 0 \tag{22}$$

where, the convection velocity U_c is set equal to the bulk velocity at the entrance.

4. Results and Discussion

The computational domain is shown in fig. 1. The main computational region is 10H×2H×7H where H is the reference height (height of cube). The inlet and the outlet are located at x=-3 and x=6, respectively. The cube is located between x=0~H, y=0~H, and z=-0.5H~0.5H. We performed calculations using two different grid sizes. In the coarse grid cases (1, 2, 3, and 4), the number of control volume is 78×42×56 in x, y, and z directions, respectively, while 106×52×74 is used for the finer grid case (5). The 'driver' region for generating inlet condition, 3H×2H×7H, is also calculated by 20×42×56 (and 30×52×74) grid points for the coarse grid cases (and finer grid case).

In the coarse grid cases (1, 2, 3, and 4), the size of grid is Δx=0.023~0.380H in the streamwise direction, Δy=0.023~0.059H in the channel height direction, and Δz=0.037~0.28H in the spanwise direction, respectively. While, in the finer grid case (5), it is Δx=0.021~0.216H, Δy=0.023~0.059H and Δz=0.024~0.31H, respectively. The size of a time marching step Δt is 0.01 H/U_m. The statistics is averaged over 20 or 30 elapse time after 60 elapse time (6000 time steps) for the coarse grid cases while it is averaged over 10 elapse time in case 5. (See table 1)

The influence of the upwind scheme was investigated using a zonal approach as follows case 1 applied the second order central difference scheme for the convective terms, case 2 applied QUICK for the entire region, and case 3 applied the QUICK scheme only in the upstream region (-3 ≤ x ≤ -0.5, 0 ≤ y≤ 2, -3.5 ≤ z ≤ 3.5) with the second order central difference in the rest of region.

Fig. 2,3 show the contours of the time averaged velocity <U> and <V> in a vertical plane through the centerline of the channel (z=0), respectively. Fig. 4,5 show the profiles of the time averaged velocity <U> and the Reynolds shear stress -<u'v'> in the centerline compared with the experimental data by Matinuzzi et al.[1].

In case 1 (S-CT) conducted with the second central difference, a wiggle propagates from the corner of the obstacle to the upstream as shown in fig. 2,3 and causes the deformation of an inlet velocity profile such that the maximum inlet velocity 〈U〉 overshoots 27% error as shown in fig. 4(a).

On the contrary QUICK suppresses the wiggle effectively in case 2 (S-QK) as shown in fig. 2,3. The error of the maximum inlet velocity 〈U〉 is reduced within 2%. However, QUICK may affect the turbulent motion obtained from the GS(grid scale) equations by introducing numerical errors. Case 2 conducted with QUICK overestimates the reversed flow region on the top of the obstacle and the flow does not reattach on the top of the obstacle. It seems that flow patterns behind the obstacle depend on the prediction of the top separation as shown in fig. 4(c). In addition, it is serious that case 2 conducted with QUICK overestimates the Reynolds stress in excess of maximum 7.6 times larger than that of experiment on the top of region and the rear of the obstacle as shown in fig. 4(b-c).

In case 3 (S-UPQK), the wiggle is restricted in the small region due to the second central difference in the front of the obstacle. It should be noted that the wiggle does not propagate behind the obstacle as shown in fig. 2,3. In case 3, the velocity profiles on the upstream region as well as the Reynolds stress profiles of the top

Table 1 Lists of calculation cases

Case	Grid number	Convective scheme	SGS model
Case 1 (S-CT)	78×42×56	2^{nd} Central	Smagorinsky
Case 2 (S-QK)	78×42×56	QUICK	Smagorinsky
Case 3 (S-UPQK)	78×42×56	QUICK (partial)	Smagorinsky
Case 4 (LDSM)	78×42×56	2^{nd} Central	Lagrangian Dynamic
Case 5 (S-CT2)	106×52×74	2^{nd} Central	Smagorinsky

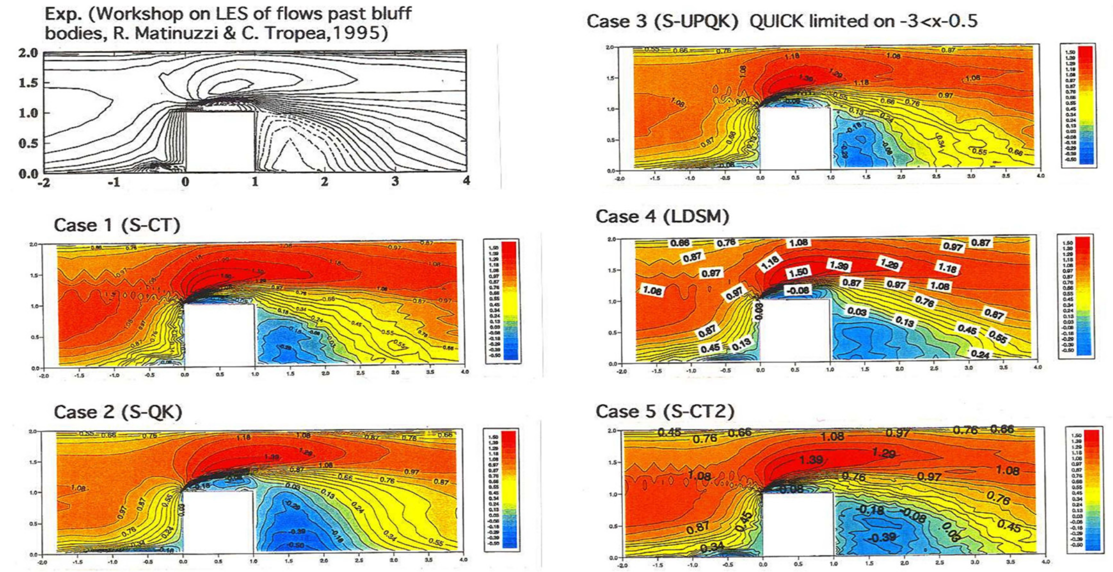

Fig. 2 Contours of the time averaged velocity <U> in a vertical plane through the centerline of the channel (z=0): (Min.=-0.5, Max.=1.5, Num.=20)

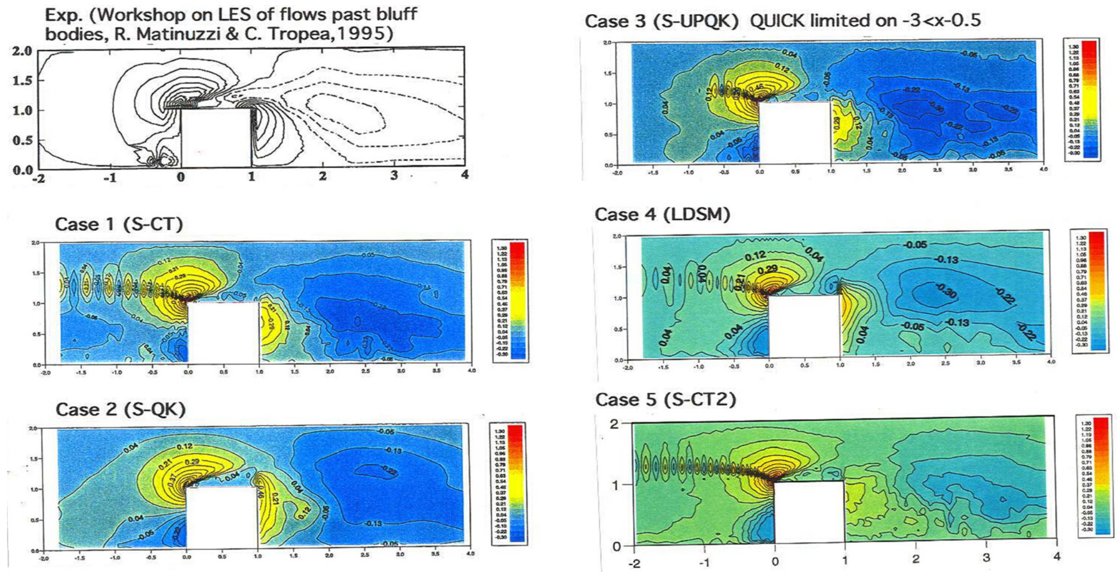

Fig. 3 Contours of the time averaged velocity <V> in a vertical plane through the centerline of the channel (z=0): (Min.=-0.3, Max.=1.3, Num.=20)

and the rear of the obstacle are improved compared with results of cases 1 and 2 as shown in fig. 3,4. A good agreement with the experiment in the case 3 indicates that the zonal adoption of QUICK scheme does not affect the flow field as opposed to usage of QUICK scheme in the entire region.

Additionally, the grid used in the case 5 is not fine enough to suppress the wiggle, although the deformation of the upstream velocity profile by wiggle is smaller than that of case 1. To obtain more improved solution in the case of the 2nd order central scheme, more spatial resolution must be required. For example, the LES with 165×65×97 grid points shows fairly good agreement with the experiment data as the result of the 'LES-Workshop of

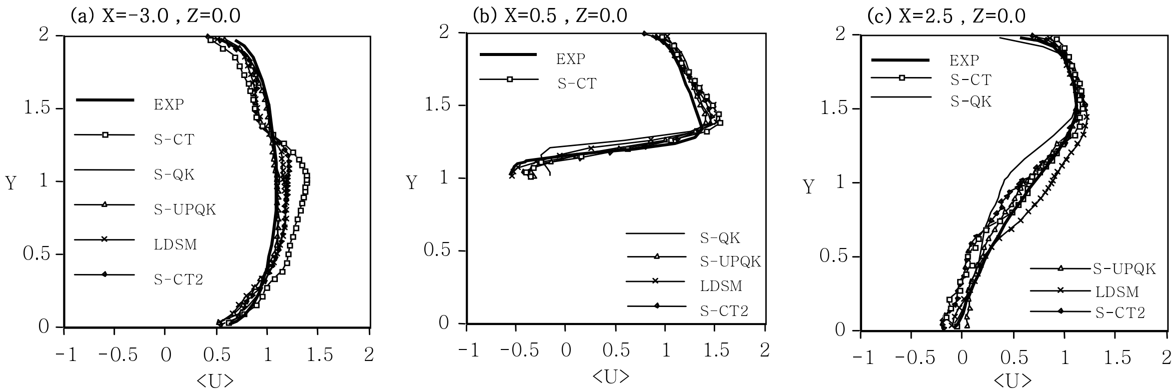

Fig. 4 Profiles of mean velocities <U> at centerline

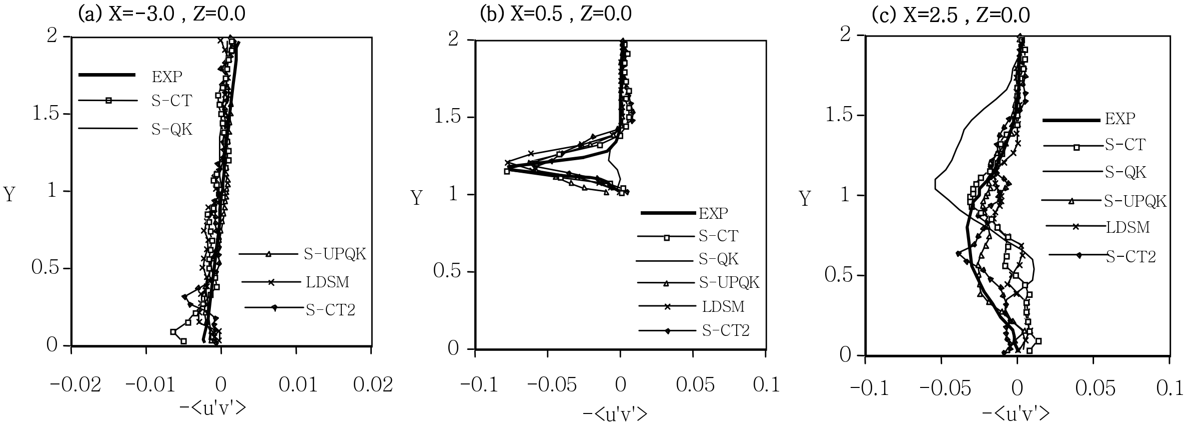

Fig. 5 Profiles of mean Reynolds shear stress -<u'v'> at centerline

Flows past Bluff Bodies'[12].

The wiggles are, however, occurred for high Reynolds numbers flow in above fine mesh LES. The wiggles are not occurred only for small Reynolds numbers (3,000) with the central scheme and no-slip condition. It is difficult to carry out fine mesh up to the wall with no-slip condition so as to keep the smallest grid within $y^+=1.0$. For this reason, QUICK scheme may be effective under careful consideration.

In Case 4 (LDSM) with the Lagrangian dynamic model conducted with the second order central difference scheme, the wiggle exists but becomes smaller than that of case 1 as shown in fig. 2 and 3 deposit of the central difference scheme. The error of the maximum velocity 〈U〉 of the inlet results in less than 6%. Fig.6 shows the contours of the Smagorinsky constant, which are predicted by LDSM. The Smagorinsky model constants in the front of the obstacle are larger than the other regions, and their magnitudes are about 0.1. The Lagrangian Dynamic SGS model automatically changes the turbulent SGS viscosity. The velocity profiles of LDSM in the upstream region are good agreement with the experiment than those of case 1 as shown in fig. 4.

Finally, the separation and the reattachment length are summarized in table 2, where X_F is the separation in the front of the cube. X_T and X_R is the reattachment length at the top and behind the cube. (See Fig. 1) Generally speaking, the QUICK tends to overestimate a separation point in the front of the obstacle.

5. CONCLUSION

The turbulent flow around the cubic obstacle mounted on a channel surface is simulated using the LES for the high Reynolds numbers 40000. In this work, the grid dependency and the effect of the QUICK are investigated

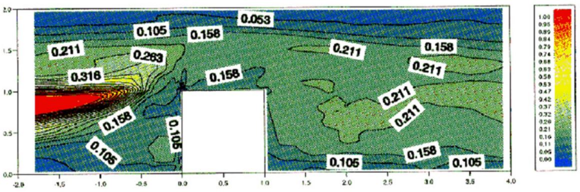

Fig. 6 Contours of Smagorinsky constant predicted by Lagrangian Dynamic SGS model at centerline plane

to verify an application of LES with a coarse mesh resolution to an engineering problem.

The wiggle occurs in the case 1 with the smallest grid size Δ_{min}=0.023 ($y^+\approx$16.6) and introduces the fatal effect to the inlet velocity ⟨U⟩ with 27% error. The inlet velocity ⟨U⟩ in the case 5 with the smallest grid size Δ_{min}=0.021 ($y^+\approx$14.5) shows 10% error. It seems that the minimum grid size attached to a solid wall to avoid the wiggle would require less than that of case 5 at least and this calculation becomes heavy inevitably for the LES of the high Reynolds flow. On the contrary, the inlet velocity ⟨U⟩ in cases 2 and 3 with QUICK is calculated within 2% error. For those reasons, usage of upwind scheme is effective in the application of the LES to practical engineering problems.

It should be note that, however, QUICK overestimates the Reynolds stress and the reversed flow region. For example, since the Reynolds stress in case 2 with QUICK becomes 7.6 times as large as that of the experiment, it results no reattachment on the top of the cube. The error of the separation length from the front side of the cube becomes 58% in case 2 while it is 39% in case3 and 20% in case1. Therefore, QUICK should not apply to the reversed flow region. In this study, local usage of QUICK in the upstream shows better agreement than usage of QUICK in the entire region.

The Lagrangian dynamic SGS model suppresses wiggles in the inlet parts without QUICK due to the local large SGS viscosity. The error of the inlet maximum velocity ⟨U⟩ of LDSM remains less than 6%. An appropriate size of time-scale is not clear for LDSM although it does

Table 2 Separation and Reattachment Length

Contrib.	X_F	X_T	X_R
Matinuzzi's Exp.	0.90	0.75	1.62
Case 1	0.72	0.89	1.83
Case 2	1.42	-	1.67
Case 3	1.25	0.89	1.47
Case 4	0.83	0.88	1.53
Case 5	0.98	0.73	1.80

not give any significant effects on simulation results in this study. Thus, LDSM is considered to be a better model than zonal adoption of QUICK in the complex turbulent flow with an obstacle.

REFERENCE

[1] 1993, Matinuzzi, R. and Tropea, C., "The Flow around Surface-mounted, Prismatic Obstacle Placed in a Fully Developed Channel Flow," *J. Fluids Engineering,* Vol.115, p.85.

[2] 1963, Smagorinsky, J.S., "General Circulation Experiments with the Primitive Equations: Part 1, basic experiments," *Monthly Weather* Rev.91, pp.99-164.

[3] 1956, Van Driest, E.R., "On Turbulent Flow near a Wall," *J. of the Aeronautical Sciences,* Vol.23, pp.1007-1011.

[4] 1991, Germano, M., Piomelli, U., Moin, P. and Cabot, W.H., "A Dynamic Subgrid Scale Eddy Viscosity Model," *Phys. Fluids,* Vol.A3, pp.1760-1765.

[5] 1992, Lilly, D.K., "A Proposed Modification of the Germano Subgrid Scale Closure Method," *Phys. Fluids,* Vol.A4, pp.633-635.

[6] 1994, Meneveau, C., Lund, T.S. and Cabot, W.H., "A Lagrangian dynamic Subgrid Scale Model for Turbulence," *CTR Proceeding of Summer Program,* pp.271-299.

[7] 1996, Tsubokura, M. and Kobayashi, T., "An Investigation of Improved Dynamic Sub-grid Scale Models by Simulating a Turbulent channel flow," *Trans. of the JSME B,* Vol.62, pp.107-114.(in Japanese)

[8] 1993, Taniguchi, N., Dai, Y. and Kobayashi, T., *9th NST symposium,* IIS, Univ. of Tokyo, Japan, pp.48-52.(in Japanese)

[9] 1975, Schumann, U., "Subgrid Scale Model for Finite Difference Simulations of Turbulence Flows in Plan Channels and Annuli," *J. Comp. Phys.,* Vol.18, pp.376-404.

[10] 1980, Williamson, J.H., "Low-Storage Runge Kutta Scheme," *Comp. Phys.,* Vol.35, p.48.

[11] 1994, Dai, Y., Kobayashi, T. and Taniguchi, N., "Large Eddy Simulation of Plane Turbulent Jet using a new outlet Velocity Boundary Condition," *JSME int. Journal B,* Vol.37, No.2, pp.242-253.

[12] 1995, Workshop on Large Eddy Simulation of Flows past Bluff Bodies (held in Tegernsee, Germany by Rodi, W. and Ferziger, J.H.), June. (not printed)